Clinical Radiology 74 (2019) 314–320

Contents lists available at ScienceDirect

Clinical Radiology

journal homepage: www.clinicalradiologyonline.net

Comparing the value of DKI and DTI in detecting isocitrate dehydrogenase genotype of astrocytomas

Y. Tan, H. Zhang*, X. Wang, J. Qin, L. Wang, G. Yang, H. Yan

Department of Radiology, First Hospital of Shanxi Medical University, Taiyuan 030001, Shanxi Province, China

ARTICLE INFORMATION

Article history:
Received 19 July 2018
Accepted 6 December 2018

AIM: To compare the value of diffusion kurtosis imaging (DKI) and diffusion tensor imaging (DTI) in evaluating astrocytomas with an isocitrate dehydrogenase (IDH) genotype.

MATERIALS AND METHODS: Fifty-eight astrocytomas were divided into IDH-wild-type (IDH-W) and IDH-mutant (IDH-M) groups, in all astrocytomas, low-grade astrocytomas (LGA) and high-grade astrocytomas (HGA), respectively. The DKI (mean kurtosis [MK], radial kurtosis [Kr], axial kurtosis [Ka]), and DTI (fractional anisotropy [FA], mean diffusivity [MD]) values were measured. The differences of parameter values between the IDH-W and IDH-M groups were compared by *t*-test. Receiver operating characteristic (ROC) curves were used to identify the best parameter and *z*-score tests were used to compare the performance between DKI and DTI.

RESULTS: In all astrocytomas, MK, Ka, and Kr values were significantly higher ($p<0.001$, $p=0.002$, and $p<0.001$), and the MD value ($p=0.005$) was lower in the IDH-W group than those in the IDH-M group. The areas under the ROC curve (AUC) of MK (0.811) and Kr (0.800) were significantly higher than that of MD (0.704). In LGA, MK, Ka, and Kr values were also significantly higher in the IDH-W group than those in the IDH-M group ($p=0.002$, $p=0.008$, $p=0.006$), whereas MD and FA values showed no differences. In HGA, MK and Kr values were significantly higher ($p=0.008$, $p=0.003$), and the MD value ($p=0.031$) was significantly lower in the IDH-W group than that in the IDH-M group, the AUC of MK (0.750) and Kr (0.788) were also higher than MD (0.637; $p=0.032$, $p=0.025$).

CONCLUSION: DKI may be a new imaging biomarker for evaluating the IDH genotype of astrocytomas, which is more accurate and stable than DTI.

Introduction

Astrocytomas are the most common type of diffuse glioma and are associated with poor prognosis.[1] Isocitrate dehydrogenase (IDH) genotype is an important prognostic marker for astrocytomas.[2,3] The presence of the IDH-mutant (IDH-M) was associated with most Grade II/III gliomas and secondary glioblastoma, which had a significantly longer overall survival than IDH-wild-type (IDH-W) tumours.[2,4] IDH-M astrocytomas are more amenable to gross total resection[5] and have better responses to standard chemo- or radiotherapy than IDH-W.[6,7] They can also be treated with targeted therapy.[8,9] Thus, early determination of IDH genotype can inform pre-treatment decision-making. Currently IDH genotype is mainly identified using

* Guarantor and correspondent: H. Zhang. Tel.: +86 18635580000.
E-mail address: zhanghui_mr@163.com (H. Zhang).

https://doi.org/10.1016/j.crad.2018.12.004
0009-9260/

immunohistochemistry or gene sequencing on tumour samples obtained invasively at biopsy or resection. Furthermore, IDH assessment based on biopsy may induce sampling bias. Non-invasive and preoperative determination of IDH genotype in routine clinical practice is urgently required.[3,10]

Magnetic resonance diffusion imaging is a technique that can measure the degree of mobility of water molecules within biological tissue. Diffusion tensor imaging (DTI) assumes that the diffusion of water molecules follows a Gaussian distribution, and it could provide a non-invasive molecular stratification of IDH for the gliomas.[11–13] The diffusion of water molecules in tumour tissue always follows a non-Gaussian distribution because of cell membrane, organelles, and water compartments. Diffusion kurtosis imaging (DKI) is the extension of DTI, which depicts the non-Gaussian distribution of water molecule diffusion and can more accurately characterise information regarding tumour heterogeneity.[14,15] DKI may be more suitable than DTI to reflect complicated water diffusion in tumour tissue.[14,15] In recent years, a few studies have indicated the superiority of DKI over DTI in detecting microstructural changes for astrocytomas grading.[16–19] DKI might be more accurate than DTI in evaluating the genotype of astrocytomas. Therefore the present study was undertaken to compare the value of DKI and DTI in evaluating IDH genotype for astrocytomas.

Materials and methods

Patients

The institutional review board of First Hospital of Shanxi Medical University approved this study protocol, and given the retrospective study and anonymous patient data, informed consent was not necessary. The patients were identified by radiology first and met the following inclusion criteria: astrocytomas newly confirmed at histopathology according to 2016 World Health Organization (WHO) criteria[2] with information regarding IDH genotype available and the scanning sequences of the patients included conventional magnetic resonance imaging (MRI) and DKI sequences. Exclusion criteria were preoperative therapy (radiotherapy, chemotherapy, or chemoradiotherapy); recurrent astrocytomas; totally cystic astrocytomas, which were difficult to draw regions of interest (ROI). Finally, 58 patients with cerebral astrocytomas (Grade II 24 cases, Grade III 15 cases, Grade IV 19 cases) were included between January 2014 and March 2017.

The patients were divided into IDH-W or IDH-M groups. To compare the stability of DTI and DKI parameters, and to test whether IDH genotype was independent of grade, comparisons between demographics and diffusion parameters were undertaken based on IDH status, independent of tumour grade (in all astrocytomas), and then on IDH status within low-grade astrocytomas (LGA, Grade II) and high-grade astrocytomas (HGA, Grade III-IV) subgroups, respectively.

MRI data acquisition

All examinations were performed using a 3 T MRI system (GE Signa HDxt, USA) using an eight-channel array coil. The imaging sequences included conventional MRI sequences (T1-weighted images [T1WI], T2-weighted images [T2WI], T2 fluid-attenuated inversion recovery [T2FLAIR], and contrast-enhanced T1WI [CE-T1WI]) and DKI sequences. The parameters of conventional MRI sequences were as follows: 195 ms repetition time (TR) and 4.76 ms echo time (TE) for gradient-echo T1WI and CE-T1WI, 4,000 ms TR and 98 ms TE for fast spin-echo T2WI, and 8,000 ms TR, 95 ms TE, and 2,000 ms interval time (TI) for T2FLAIR. Section thickness and interval were 5/1.5 mm; field of view (FOV) was 240×240 mm. Gadolinium chelate 0.1 mmol/kg body weight was used as the contrast medium.

Echo planar imaging (EPI) was used to obtain DKI data. Implemented b-values were 0, 1,000, and 2,000 mm^2/s. These were applied in 30 uniformly distributed directions. The following imaging parameters were kept constant throughout the DKI data (including DTI data) acquisition sequences: 6,500 ms TR, 11 ms TE; 240×240 mm FOV, 96×96 matrix, number of signals acquired=1; the section thickness and interval were 6/1 mm. The scan time of DKI was approximately 7 minutes.

MRI data processing and analyses

DKI software in GE Functool 9.4.05a was used to perform DKI analysis on GE Advanced Workstation 4.4. The DKI data were corrected for eddy current distortions and head motion by global affine transformations. The diffusion tensor and diffusion kurtosis were calculated on a voxel-by-voxel basis and all data (b=0, 1,000, and 2,000 mm^2/s) were used. After the kurtosis and diffusion tensor were estimated by fitting all DWIs into equation (1), five metrics could be derived from the two tensors, including DKI parameters: mean kurtosis (MK), radial kurtosis (Kr), axial kurtosis (Ka), and DTI parameters: mean diffusivity (MD), fractional anisotropy (FA).[18,19] MK reflects the degree of water diffusion deviation from the Gaussian curve. Ka reflects the kurtosis value along the axial direction of the DTI ellipsoid. Kr reflects the average value of all diffusion kurtosis, which is perpendicular to the main direction of diffusion. MD reflects the overall level of water molecules diffusion and the diffusion resistance. FA reflects the ratio of water diffusion anisotropy composition with the entire diffusion tensor.[18,19]

$$\ln[S(n,b)/S_0] = -b\sum_{i=1}^{3}\sum_{j=1}^{3} n_i n_j D_{ij} + \frac{1}{6}b^2\overline{D}^2\sum_{i=1}^{3}\sum_{j=1}^{3}\sum_{k=1}^{3} \times \sum_{l=1}^{3} n_i n_j n_k n_l W_{ijkl} \quad (1)$$

here, $S(n,b)$ is diffusion direction n and b-value b can be approximated by kurtosis and diffusion tensor, S_0 is the signal intensity for b0 image, $D(\_)$ is the mean diffusivity, n_i (i=1,2,3) is the component of the diffusion direction vector

n. W_{ijkl} and D_{ij} are the components of the kurtosis and diffusion tensor, respectively.

Conventional MRI sequences were used to visualize the basic features of tumours, such as cystic, necrotic, and haemorrhagic components, tumoural solid parts, tumour boundaries, and range of oedema, which were used to determine the ROI. The ROIs of tumoural solid parts were drawn manually on one conventional image and marked automatically on MK, Kr, Ka, MD, and FA images by the DKI software in GE Functool 9.4.05a. The parameter values in the tumoural solid parts are mainly dependent on the tumour itself rather than individual white matter, which is destroyed and replaced by tumour tissue, and the influence of individual differences is negligible.[18,19] Therefore, the parameters were not normalized by the value of contralateral normal white matter.

ROIs of enhanced parts of the tumours, which represented the solid parts, were delineated on transverse CE-T1WI by excluding the necrotic, cystic, haemorrhagic components, and adjacent normal tissue, which prevented the partial volume effect. ROIs of solid parts of unenhanced tumours were delineated on transverse T2WI, by excluding the adjacent normal tissue and peritumoural oedema according to T2FLAIR imaging. The intensity of solid parts of unenhanced tumours was lower than peritumoural oedema on T2FLAIR imaging, and higher on DWI. Two independent neuroradiologists (with 15 and 8 years of experience) blinded to the pathological results performed image analysis, and measured each parameter value on the solid parts of tumours three times, followed by the calculation of total mean value of each parameter for each patient, which ensured the parameter values were more accurate.

IDH analysis in astrocytoma

IDH-M status of astrocytomas was determined using Sanger sequencing. DNA was extracted from paraffin blocks using a Simlex OUP® FFPE DNA kit (TIB, Germany). Genes were amplified by PCR ABI9700 life technologies (Thermo Fisher Scientific, USA). IDH-M of astrocytomas includes IDH1-M and IDH2-M. Gene-specific primers (Primer-blast, NCBI) of IDH1 were forward (F): 5′–CGGTCTTCAGAGAAGCCATT–3′, reverse (R): 5′–GCA AAATCACATTATTGCCAA–3′; and, for IDH2, were F: 5′–CAAGAGGATGGCTAGGCGAG–3′, R: 5′–CAAGC TGAAGAAGATGTGGAAAAG–3′. Sanger sequencing was performed by ABI3500 life technologies (Thermo Fisher Scientific).

Statistical analysis

SPSS version 18.0 statistical software was used for data analyses. Inter-group differences between IDH-W and IDH-M groups with respect to the DKI parameters (MK, Kr, and Ka) and DTI parameters (MD and FA) values in the solid parts of the tumours were compared using the t-test. $p<0.05$ was considered statistically significant. Receiver operating characteristic (ROC) curves were generated for DKI (MK, Kr, and Ka) and DTI (MD and FA) parameter values to select the best parameter. To compare the value of DKI and DTI parameters in evaluating IDH genotype, a z-score test was used.

Result

Patient groups

The patients' characteristics were showed in Table 1. The IDH-M genotype was identified in 27 of 58 (46.55%) astrocytomas. Seventeen cases of IDH-M were identified out of 24 (70.83%) LGA, and 10 out of 34 (29.41%) HGA of which six were Grade III, and four were Grade IV. The study population comprised 31 men and 27 women. The mean age of the astrocytoma patients within the IDH-W and IDH-M groups was 55.19±1.2 and 41.52±1.1 years, respectively, and there was an obvious statistical difference ($p<0.001$). LGA patients with IDH-W were older than patients with IDH-M, but there was no statistical difference ($p=0.097$). HGA patients with IDH-W were significantly older than patients with IDH-M ($p=0.001$).

In all astrocytomas

DKI parameter values (MK, Kr, and Ka) and DTI parameter values (MD and FA) of astrocytomas are shown in Table 2 and Figs 1 and 2. The MK, Ka, and Kr values in the solid parts of the tumours were significantly higher ($p<0.001$, $p=0.002$, and $p<0.001$, respectively), and the MD value was significantly lower in the IDH-W group compared to those in the IDH-M group ($p=0.005$). The FA value did not differ significantly between groups. The area under the ROC curve (AUC) of MK, Kr, Ka, and MD values was 0.811 (95% confidence interval [CI]: 0.700–0.923), 0.800 (95% CI: 0.688–0.913), 0.750 (95% CI: 0.614–0.886), 0.704 (95% CI: 0.568–0.840), and the cut-off value was 0.393, 0.351, 0.379, 0.455, respectively. The AUC of MK and Kr was significantly higher than that of MD ($p=0.037$, $p=0.043$, respectively). The optimal threshold, sensitivity, and specificity associated

Table 1
The clinical characteristics of patients.

	All astrocytomas (N=58)			Low-grade (N=24)			High-grade (N=34)		
	IDH-W (N=31)	IDH-M (N=27)	*p-value*	IDH-W (N=7)	IDH-M (N=17)	*p-value*	IDH-W (N=24)	IDH-M (N=10)	*p-value*
Age (Years)	55.19±1.2	41.52±1.1	<0.001	50.9±1.4	41.9±1.1	0.097	56.5±1.2	40.9±1.1	0.001
Gender (M/F)	18/13	13/14	-	3/4	7/10	-	15/9	6/4	-

Table 2
DKI and DTI parameter values of patients in all, low-grade and high-grade astrocytomas.

Parameter	All astrocytomas			Low-grade astrocytomas			High-grade astrocytomas		
	IDH-W (N=31)	IDH-M (N=27)	*p-value*	IDH-W (N=7)	IDH-M (N=17)	*p-value*	IDH-W (N=24)	IDH-M (N=10)	*p-value*
MK	0.67±0.13	0.48±0.16	<0.001	0.68±0.11	0.47 ±0.13	0.002	0.66±0.14	0.49±0.20	0.008
Kr	0.68±0.19	0.45±0.18	<0.001	0.67±0.16	0.47±0.14	0.006	0.68±0.20	0.43±0.18	0.003
Ka	0.66±0.14	0.53±0.17	0.002	0.66±0.11	0.49±0.14	0.008	0.66±0.15	0.60±0.20	0.330
MD	1.22±0.26	1.49±0.41	0. 005	1.23±0.28	1.46±0.30	0.103	1.22±0.27	1.54±0.57	0. 031
FA	0.20±0.09	0.18±0.17	0.408	0.21±0.10	0.17±0.04	0.144	0.20±0.08	0.20±010	0.865

DKI, diffusion kurtosis imaging; DTI, diffusion tension imaging; MK, mean kurtosis; Kr, radial kurtosis; Ka, axial kurtosis; MD, mean diffusivity; FA, fractional anisotropy.

with each parameter are shown in Table 3 and the ROC curves are shown in Fig 3.

In LGA

The MK, Ka, and Kr values were significantly higher (p=0.002, p=0.008, and p=0.006, respectively) in the IDH-W group than IDH-M group, and the MD and FA values did not differ significantly between two groups (Table 2). The AUC of MK, Kr, and Ka values was 0.857 (95% CI: 0.692–1.023), 0.857 (95% CI: 0.665–1.049), 0.849 (95% CI: 0.695–1.003), and the cut-off values were 0.355, 0.346, 0.353, respectively (Table 3; Fig 3).

In HGA

The MK and Kr values were significantly higher (p=0.008, and p=0.003), and the MD value (p=0.031) was significantly lower in the IDH-W group compared to that in the IDH-M group. The Ka and FA values did not differ significantly between the two groups (Table 2). The AUCs of the MK, Kr, and MD values were 0.750 (95% CI: 0.556–0.944), 0.788 (95% CI: 0.624–0.951), 0.673 (95% CI: 0.465–0.881), and the cut-off values were 0.393, 0.351, 0.455, respectively (Table 3; Fig 3). The AUC of MK and Kr was significantly higher than that of MD (p=0.032, p=0.025, respectively).

Discussion

IDH-M astrocytomas are more amenable to gross total resection[5] and more sensitive to radio chemotherapy than IDH-W tumours,[6–9] which resulted in a longer overall survival for IDH-M astrocytomas compared to IDH-W.[2] Thus, the accurate evaluation of IDH genotype for glioma is particularly important regarding pre-treatment decision-making. In the present study, the results demonstrated that the MK, Kr, Ka, and MD values enabled differentiation of IDH-W from IDH-M astrocytomas. Furthermore, MK and Kr obtained from DKI had greater diagnostic value than MD in detecting the IDH genotype. DKI may be a new imaging biomarker for evaluating IDH genotype in astrocytomas, which is more accurate and stable than DTI.

The present results showed that MK, Ka, and Kr values in the solid parts of the tumours were significantly higher in the IDH-W group as compared to that in the IDH-M group; this is consistent with other studies.[20–22] It has been confirmed that IDH mutation could convert α-ketoglutarate to 2-hydroxyglutarate and decrease the levels of hypoxia-inducible factor 1α,[23,24] which ultimately suppressed

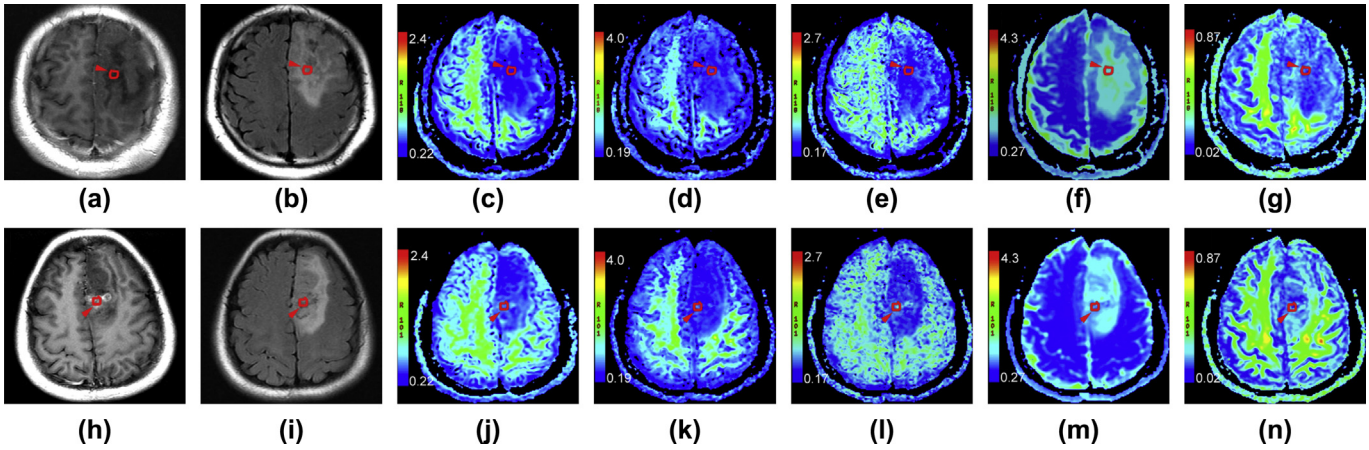

Figure 1 Grade II astrocytomas. A–G: 44-year-old woman with astrocytoma IDH-M. The tumour in the left frontal lobe showed no enhancement on enhanced T1WI (A), and iso-intensity on T2FLAIR (B). MK (C), Kr (D), Ka (E) and FA (G) maps showed hypointensity, MD map (F) showed hyperintensity; H–N: 33-year-old man with astrocytoma IDH-W. The tumour showed small pieces of enhancement on enhanced T1WI (H), and iso-intensity on T2FLAIR (I). MK (J), Kr (K), Ka (L) and FA (N) map shows hyperintensity, MD map (M) showed hypointensity. The red curves and arrows represented the ROI of solid parts of the tumours.

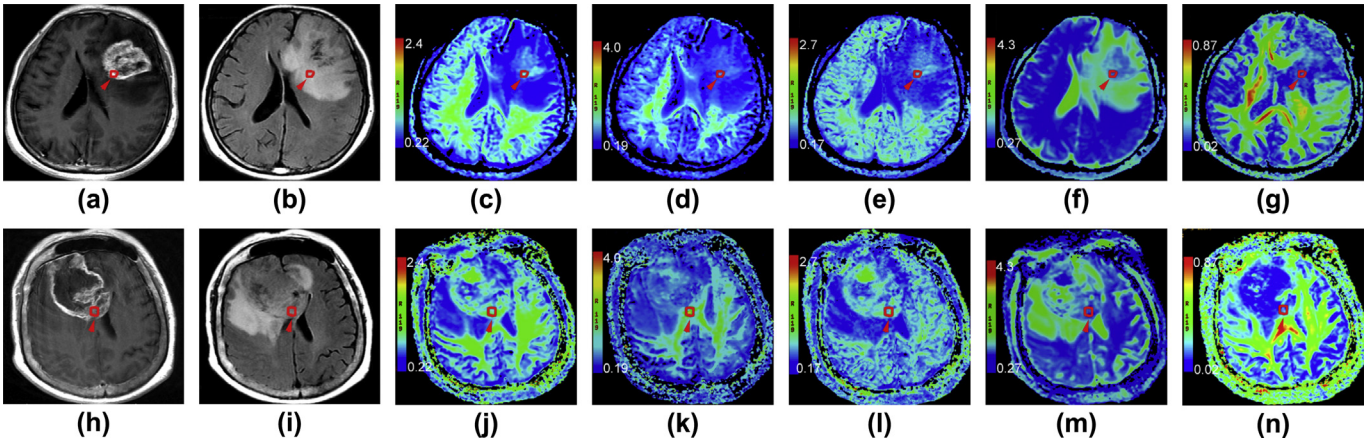

Figure 2 Grade IV astrocytomas. A–G: 62-year-old woman with astrocytoma IDH-M. The tumour in the left frontal lobe shows obvious enhancement on enhanced T1WI (A), and heterogeneous intensity on T2FLAIR (B). MK (C), Kr (D), and Ka (E) maps showed slight hyperintensity, MD (F) and FA (G) maps showed hypointensity; H–N: 59-year-old woman with astrocytoma IDH-W. The tumour in the right frontal lobe showed obvious enhancement on enhanced T1WI (G), and heterogeneous intensity on T2FLAIR (I). MK (J), Kr (K), Ka (L) map shows obvious hyperintensity, MD (M)and FA (N) map showed hypointensity. The red curves and arrows represented the ROI of solid parts of the tumours.

aggressive behaviour, such as angiogenesis and cell proliferation in gliomas.[25] This suggests that the structure of IDH-W astrocytomas is more complex than IDH-M astrocytomas because of increased tumour angiogenesis, greater nuclear atypia, and higher cell density. As an advanced diffusion imaging sequence, DKI can provide additional kurtosis information, which might characterise the heterogeneity of the microenvironment.[18,19] Greater DKI parameter values indicate more complex structures in the tumour.[21] Thus, DKI could reflect the difference in heterogeneity between IDH-W and IDH-M astrocytomas.

By performing ROC analyses, the MK and Kr parameters of DKI were found to have a significantly better diagnostic performance than MD and FA derived from DTI. There may be two explanations for this result. The first is that the diffusion of water molecules *in vivo* always follows non-Gaussian distribution because of cell membranes and organelles.[18,19] DKI can characterise non-Gaussian distribution of water molecule diffusion and quantify the deviation from Gaussian diffusion, while the theoretical assumption of DTI is that the diffusion of water molecules follows a Gaussian distribution.[20–22] DKI could reflect the real situation of water molecule movement in tumour tissue and be accurate enough to characterise the heterogeneity of tumours. Previous studies also showed that DKI was better than DTI in tumour grading[18] and differential diagnosis[19] for glioma. The other one is that DKI is more accurate and sensitive for the detection of microstructural changes such as tracking pathological processes[26] or the white matter fibers changes of Parkinson's disease.[27] Furthermore, when restricting our patients into low-grade or high-grade astrocytomas for predicting IDH genotype, the diagnostic performances of MK and Kr are much better than MD both in LGA and HGA subgroups. These findings further attested to the higher stability of DKI in detecting micro-structural changes than DTI. We confirmed our hypothesis that DKI was more accurate and stable than DTI to evaluate IDH genotype of astrocytoma.

In this study we also have found that the DKI parameter values of IDH-W LGA was higher than that of IDH-M HGA. This is consistent with previous studies. Tan[28] has found that the rCBV ratio of Grade II IDH-W astrocytomas was higher than that of Grade III IDH-M astrocytomas. Hartmann[3] has showed that the survival time of IDH-M glioblastomas was longer than that of IDH-W anaplastic astrocytomas. Reuss[29] found that Grade II IDH-W astrocytoma and Grade III IDH-M astrocytoma represented virtually identical groups in respect to the age and overall survival of patients. Furthermore, most of the gliomas classified as IDH-W astrocytomas can be allocated to other tumour entities on a molecular basis, and they most likely represent glioblastomas.[30] So IDH genotype might have

Table 3
ROC analysis of DKI and DTI parameter values in predicting IDH genotype.

Parameter	All astrocytomas					Low-grade astrocytomas					High-grade astrocytomas				
	Cut-off	Sensitivity	Specificity	AUC	*p-value*	Cut-off	Sensitivity	Specificity	AUC	*p-value*	Cut-off	Sensitivity	Specificity	AUC	*p-value*
MK	0.393	100%	85.2%	0.811	<0.001	0.355	100%	88.2%	0.857	0.007	0.419	100%	60%	0.750	0.023
Kr	0.351	96.8%	85.2%	0.800	<0.001	0.346	100%	76.5%	0.857	0.007	0.362	95.8%	60%	0.788	0.009
Ka	0.379	100%	81.5%	0.750	0.001	0.353	100%	82.4%	0.849	0.008	-	-	-	0.600	0.364
MD	0.455	100%	92.6%	0.704	0.008	-	-	-	0.311	0.153	-	-	-	0.673	0.117

ROC, Receiver operating characteristic; DKI, diffusion kurtosis imaging; DTI, diffusion tension imaging; MK, mean kurtosis; Kr, radial kurtosis; Ka, axial kurtosis; MD, mean diffusivity; AUC, area under the curve.

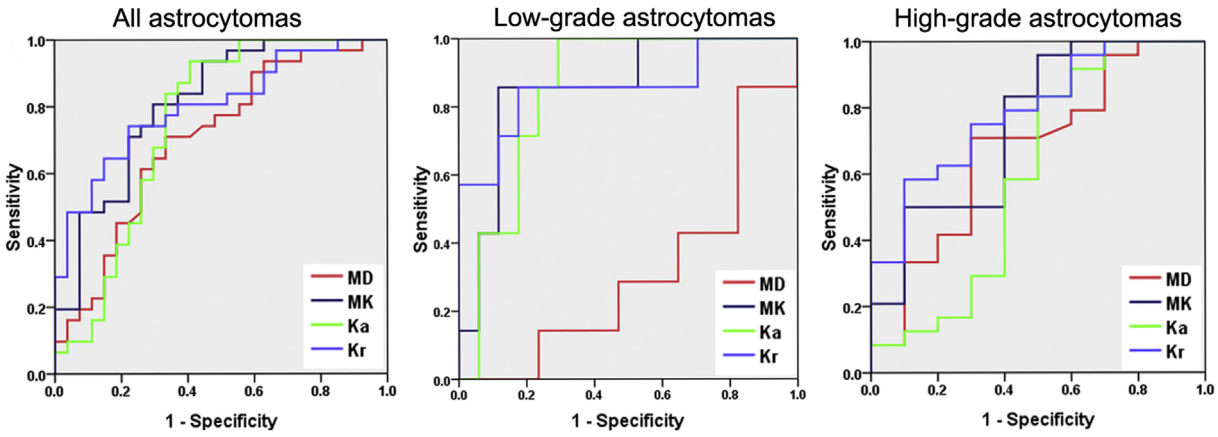

Figure 3 ROC analysis of DKI and DTI parameter values in predicting IDH genotype.

more significant prognostic value than tumour grading for astrocytomas.

The current study has several limitations. First, the retrospective case selection, the pathological proof in the area where the ROI selected could not be supplied. But all the pathological examinations were performed by one experienced pathologist to make sure the higher-grade region was selected. Second, these are preliminary findings that will need to be validated in future studies. Third, proliferation and angiogenesis of tumour tissue was not analysed for histological examination in our study. Lastly, the relatively small sample size was another limitation in our study. Further studies with a larger sample of patients with cerebral astrocytomas are planned.

In conclusion, DKI may be a new imaging biomarker for evaluating IDH genotype in astrocytomas, which is better and more stable than DTI.

Acknowledgements and Disclosure

This study has received funding by the National Natural Science Foundation (81471652 and 81771824 to Hui Zhang; 81701681 to Yan Tan; 11705112 to Guo-qiang Yang); grants from the Precision Medicine Key Innovation Team Project to Hui Zhang (YT1601); grants from the Social Development Projects of Key R&D program in Shanxi Province to Hui Zhang (201703D321016); grants from the Natural Science Foundation of Shanxi Province to Yan Tan (201601D021162). The authors declare that they have no conflict of interest.

References

1. Ichimura K, Narita Y, Hawkins CE. Diffusely infiltrating astrocytomas: pathology, molecular mechanisms and markers. *Acta Neuropathol* 2015;**129**(6):789–808.
2. Louis DN, Perry A, Reifenberger G, *et al*. The 2016 world health organization classification of tumours of the central nervous system: a summary. *Acta Neuropathol* 2016;**131**(6):803–20.
3. Hartmann C, Hentschel B, Wick W, *et al*. Patients with IDH1 wild type anaplastic astrocytomas exhibit worse prognosis than IDH1-mutated glioblastomas, and IDH1 mutation status accounts for the unfavorable prognostic effect of higher age: implications for classification of gliomas. *Acta Neuropathol* 2010;**120**(6):707–18.
4. Yu J, Shi Z, Lian Y, *et al*. Noninvasive IDH1 mutation estimation based on a quantitative radiomics approach for grade II glioma. *Eur Radiol* 2017;**27**(8):3509–22.
5. Beiko J, Suki D, Hess KR, *et al*. IDH1 mutant malignant astrocytomas are more amenable to surgical resection and have a survival benefit associated with maximal surgical resection. *Neuro Oncol* 2014;**16**(1):81–91.
6. Kizilbash SH, Giannini C, Voss JS, *et al*. The impact of concurrent temozolomide with adjuvant radiation and IDH mutation status among patients with anaplastic astrocytoma. *J Neurooncol* 2014;**120**(1):85–93.
7. Tran AN, Lai A, Li S, *et al*. Increased sensitivity to radiochemotherapy in IDH1 mutant glioblastoma as demonstrated by serial quantitative MR volumetry. *Neuro Oncol* 2016;**16**(3):414–20.
8. Rohle D, Popovici-Muller J, Palaskas N, *et al*. An inhibitor of mutant IDH1 delays growth and promotes differentiation of glioma cells. *Science* 2013;**340**(6132):626–30.
9. Waitkus MS, Dilpas BH, Yan H. Biological role and therapeutic potential of IDH mutation in cancer. *Cancer Cell* 2018, https://doi.org/10.1061/j.ccell.2-18.04.011.
10. Flavahan WA, Drier Y, Liau BB, *et al*. Insulator dysfunction and oncogene activation in IDH mutant gliomas. *Nature* 2016;**529**(7584):110–4.
11. Xiong J, Tan W, Wen J, *et al*. Combination of diffusion tensor imaging and conventional MRI correlates with isocitrate dehydrogenase 1/2 mutations but not 1p/19q genotyping in oligodendroglial tumours. *Eur Radiol* 2016;**26**(6):1705–15.
12. Roettger D, Yuan JL, Mancini L, *et al*. The role of diffusion tensor imaging for non-invasive IDH phenotyping in gliomas. *J Clin Oncol* 2018, https://doi.org/10.1200/JCO.2018.36.15.
13. Price SJ, Allinson K, Liu H, *et al*. Less invasive phenotype found in isocitrate dehydrogenase mutated glioblastomas than in isocitrate dehydrogenase wild-type glioblastomas: a diffusion-tensor imaging study. *Radiology* 2017;**283**(1):215–21.
14. Hui ES, Fieremans E, Jensen JH, *et al*. Stroke assessment with diffusional kurtosis imaging. *Stroke* 2012;**43**(11):2968–73.
15. Zheng WB, Wu CX, Huang LX, *et al*. Diffusion kurtosis imaging of microstructural alterations in the brains of paediatric patients with congenital sensorineural hearing loss. *Sci Rep* 2017;**7**(1):1543.
16. Raab P, Hattingen E, Franz K, *et al*. Cerebral gliomas: diffusional kurtosis imaging analysis of microstructural differences. *Radiology* 2010;**254**(3):876–81.
17. Van Cauter S, De Keyzer F, Sima DM, *et al*. Integrating diffusion kurtosis imaging, dynamic susceptibility-weighted contrast-enhanced MRI, and short echo time chemical shift imaging for grading gliomas. *Neuro Oncol* 2014;**16**(7):1010–21.
18. Tan Y, Zhang H, Zhao RF, *et al*. Comparison of the values of MRI diffusion kurtosis imaging and diffusion tensor imaging in cerebral astrocytoma grading and their association with aquaporin-4. *Neurol India* 2016;**64**(2):265–72.
19. Tan Y, Wang XH, Zhang H, *et al*. Differentiation of high-grade-astrocytomas from solitary-brain-metastases: comparing diffusion kurtosis imaging and diffusion tensor imaging. *Eur J Radiol* 2015;**84**(12):2618–24.

20. Hempela JM, Schittenhelmb J, Bisdasc S, *et al*. In vivo assessment of tumour heterogeneity in WHO 2016 glioma grades using diffusion kurtosis imaging: diagnostic performance and improvement of feasibility in routine clinical practice. *J Neuroradiol* 2018;**45**(1):32–40.
21. Hempela JM, Schittenhelmb J, Bisdasc S, *et al*. Effect of perfusion on diffusion kurtosis imaging estimates for in vivo assessment of integrated 2016 WHO glioma grades. *Clin Neuroradiol* 2017, https://doi.org/10.1007/s00062-017-0606-8.
22. Hempela JM, Bisdasc S, Schittenhelm J, *et al*. In vivo molecular profiling of human glioma using diffusion kurtosis imaging. *J Neurooncol* 2017;**131**(1):93–101.
23. Masui K, Kato Y, Sawada T, *et al*. Molecular and genetic determinants of glioma cell invasion. *Int J Mol Sci* 2017;**18**(12):E2609.
24. Parsons DW, Jones S, Zhang X, *et al*. An integrated genomic analysis of human glioblastoma multiforme. *Science* 2008;**321**(5897):1807–12.
25. Dang L, Yen K, Attar EC. IDH mutations in cancer and progress toward development of targeted therapeutics. *Ann Oncol* 2016;**27**(4):599–608.
26. Bar-Shir A, Duncan ID, Cohen Y. QSI and DTI of excised brains of the myelin-deficient rat. *Neuroimage* 2009;**48**(1):109–16.
27. Kamagata K, Tomiyama H, Hatano T, *et al*. A preliminary diffusional kurtosis imaging study of Parkinson disease: comparison with conventional diffusion tensor imaging. *Neuroradiology* 2014;**56**(3):251–8.
28. Tan W, Xiong J, Huang W, *et al*. Noninvasively detecting isocitrate dehydrogenase 1 gene status in astrocytoma by dynamic susceptibility contrast MRI. *J Magn Reson Imaging* 2017;**45**(2):492–9.
29. Reuss DE, Mamatjan Y, Schrimpf D, *et al*. IDH mutant diffuse and anaplastic astrocytomas have similar age at presentation and little difference in survival: a grading problem for WHO. *Acta Neuropathol* 2015;**129**(6):867–73.
30. Reuss DE, Kratz A, Sahm F, *et al*. Wild type astrocytomas biologically and clinically resolve into other tumour entities. *Acta Neuropathol* 2015;**130**(3):407–17.